Entropy of weighted recurrence plots

Deniz Eroglu,[1,2,*] Thomas K. DM. Peron,[3,†] Nobert Marwan,[1] Francisco A. Rodrigues,[4] Luciano da F. Costa,[3] Michael Sebek,[5] István Z. Kiss,[5] and Jürgen Kurths[1,2,6]

[1]*Potsdam Institute for Climate Impact Research, 14473 Potsdam, Germany*

[2]*Department of Physics, Humboldt University, 12489 Berlin, Germany*

[3]*Instituto de Física de São Carlos, Universidade de São Paulo, 13566-590 São Carlos, São Paulo, Brazil*

[4]*Departamento de Matemática Aplicada e Estatística, Instituto de Ciências Matemáticas e de Computação,Universidade de São Paulo, Caixa Postal 668,13560-970 São Carlos, São Paulo, Brazil*

[5]*Department of Chemistry, Saint Louis University, 3501 Laclede Avenue, St. Louis, Missouri 63103, USA*

[6]*Institute for Complex Systems and Mathematical Biology, University of Aberdeen, Aberdeen AB24 3UE, United Kingdom*

(Received 9 July 2014; published 21 October 2014)

The Shannon entropy of a time series is a standard measure to assess the complexity of a dynamical process and can be used to quantify transitions between different dynamical regimes. An alternative way of quantifying complexity is based on state recurrences, such as those available in recurrence quantification analysis. Although varying definitions for recurrence-based entropies have been suggested so far, for some cases they reveal inconsistent results. Here we suggest a method based on weighted recurrence plots and show that the associated Shannon entropy is positively correlated with the largest Lyapunov exponent. We demonstrate the potential on a prototypical example as well as on experimental data of a chemical experiment.

DOI: 10.1103/PhysRevE.90.042919 PACS number(s): 89.75.Kd, 89.75.Hc

I. INTRODUCTION

First conceived to visualize the time-dependent behavior of complex dynamical systems, recurrence plots (RPs) have been shown to be a powerful technique to uncover statistically many characteristic properties of such systems [1,2]. A crucial issue in the study of time series originating from complex systems is the detection of dynamical transitions, a task that RPs have been accomplishing due to a set of RP-based measures of complexity. Examples of their successful application in real-world systems can be found in neuroscience [3–5], earth science [6–9], astrophysics [10–12], and other areas of research [13].

The measures defined by the RP framework, called recurrence quantification analysis (RQA), are based on point density and the length of diagonal and vertical line structures visible in the RP, which are regarded as alternative measures to quantify the complexity of physical systems. In order to the uncover time-dependent behavior of nonlinear time series, RQA measures are often computed by setting sliding time windows, which then can be used to identify dynamical transitions, such as periodic to chaos transitions [14] and even chaos-chaos transitions [15].

Since the calculation of Lyapunov exponents is often infeasible for systems whose equations of motion are not accessible, various estimators for measuring the divergence behavior of dynamical systems have been suggested. Entropy based quantifiers of RPs, e.g., the normalized entropy of recurrence times [16–18] or the Shannon entropy of the distribution of length of diagonal line segments [14], are able to detect points of bifurcation.

However, the entropy of the diagonal line segments reveals, for some cases, a counterintuitive anticorrelation with the Lyapunov exponent, yielding high values within periodic windows and low values within chaotic regimes [14]. To solve this apparent contradiction between the notion of disorganization of a system and the value of the line length entropy [14], another definition for a recurrence-based entropy has been suggested, employing the nonrecurrent (white) diagonal lines in the RP [19]. It is important to emphasize that these definitions do not correspond to the entropy of physical systems in a classical statistical physics sense [13].

The property of recurrence is often represented by an unweighted RP, i.e., a binary matrix whose elements indicate that two points are recurrent, once the distance between them is below a certain threshold [2]. The restriction of unweighted RPs naturally introduces a free parameter in the analysis given by the distance threshold. Here we present an alternative definition of a RP-based entropy, by using a weighted variant of the RP. More specifically, here we relax the condition of defining distance thresholds by introducing the Shannon entropy of weighted recurrence plots (WRPs), which is only based on the distances between the points in the phase space. We illustrate this concept on time series generated by the logistic map and Rössler oscillator, showing that, in contrast to the line length entropy, the entropy derived from WRPs has a stable behavior through the range of bifurcation parameters. Furthermore, we show that this definition is also positively correlated with the Lyapunov exponent. An application to time series from chemical oscillators demonstrates the potential for studies of real-world experiments. Finally, we summarize the differences, potentials, and pitfalls between the different recurrence-based entropies.

This paper is organized as follows. In Sec. II we define RPs and WRPs and review the definitions of the recurrence-based Shannon entropies. Section III is devoted to the comparison of different definitions of recurrence entropies for model systems and experimental data. We summarize and give our conclusions in Sec. IV.

*eroglu@pik-potsdam.de

†thomas.peron@usp.br

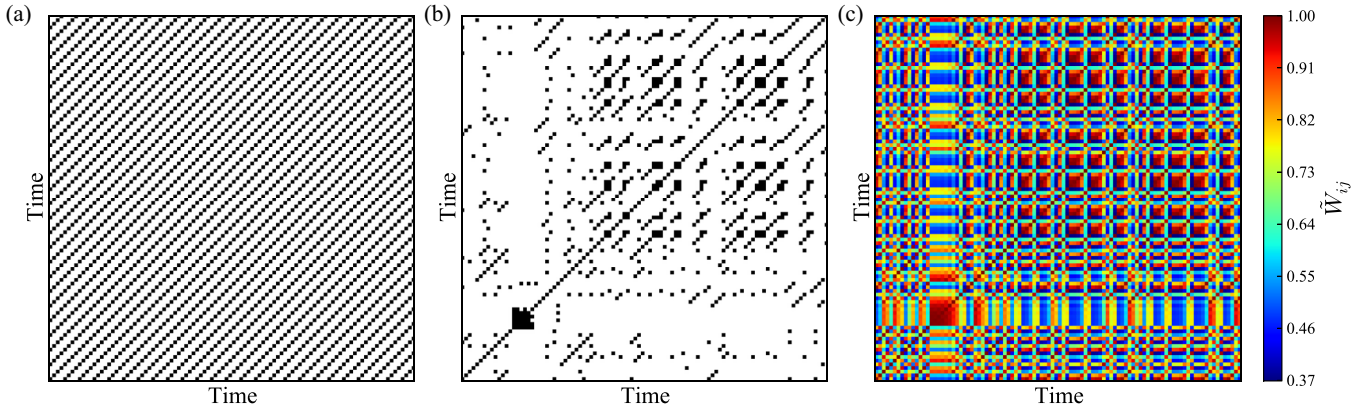

FIG. 1. (Color online) Recurrence plot of logistic map for (a) $r = 3.5$ (periodic regime) and (b) $r = 4.0$ (chaotic regime) and (c) weighted recurrence plot of logistic map for $r = 4.0$ (chaotic regime).

II. RECURRENCE PLOTS AND ENTROPY

In a given m-dimensional phase space, two points are considered to be recurrent if their state vectors lie in a neighborhood characterized by a threshold ε. Formally, for a given trajectory $\mathbf{x}_i$ $(i = 1, \ldots, N, \mathbf{x} \in \mathbb{R}^m)$, the recurrence matrix $\mathbf{R}$ is defined as

$$R_{i,j}(\varepsilon) = \Theta(\varepsilon - \|\mathbf{x}_i - \mathbf{x}_j\|), \quad i, j = 1, \ldots, N, \tag{1}$$

where N is the trajectory length, $\Theta(\cdot)$ is the Heaviside function, and $\|\cdot\|$ is the Euclidean norm of the adopted phase space [2]. In a RP, elements $R_{i,j} \equiv 1$ (recurrence) are usually said to be black dots, whereas $R_{i,j} \equiv 0$ (no recurrence) are usually called white dots [Figs. 1(a) and 1(b)]. The trajectory phase space can be reconstructed via time-delay embedding for a time series $\{u_i\}_{i=1}^{N}$ [20],

$$\mathbf{x}_i = (u_i, u_{i+\tau}, \ldots, u_{i+\tau(m-1)}), \tag{2}$$

where m is the embedding dimension and τ is the embedding delay. The dimension m can be found by nearest neighbors and the delay τ by mutual information or autocorrelation [21].

The main diagonal of $\mathbf{R}$, $R_{i,i} \equiv 1 \forall i$, shows the line of identity (LOI). The RP is a symmetric and binary matrix. The motifs of line segments in a RP occur according to the dynamical patterns of the underlying system. If the dynamics is a uniformly distributed white noise, homogeneously distributed black points are observed. If the system is deterministic, the matrix displays diagonal line segments of black dots. The length of these diagonals is related to the divergence of the trajectories and is associated with the dynamics of the system. Due to this intrinsic relationship between the system's dynamics and the distribution of line segments in RPs, measures of complexity based on line segments have been introduced in order to study the dynamical properties of different systems [2,14].

Measures based on the length ℓ of the diagonal in the recurrence matrices ($R_{i,j} = 1$) are often used to quantify the complexity of a given RP. As we have mentioned before, the distribution of diagonal line lengths $P(\ell)$ is linked to the maximum Lyapunov exponent, since $P(\ell)$ can be considered a quantification of the divergence behavior of the dynamical system that originated the RP [2,22]. Among other measures introduced within the RQA, the diagonal-line-based entropy was empirically derived [13,14] by measuring the complexity and variability of the occurring diagonal lines formed from recurrence points [2], i.e.,

$$S_{\mathrm{RP}} = -\sum_{\ell=\ell_{\min}}^{\ell_{\max}} p(\ell) \ln p(\ell), \tag{3}$$

where $\ell_{\max}$ is the length of the longest diagonal line, $p(\ell) = P(\ell)/N_\ell$ is the probability of occurrence of a line of length ℓ, and N_ℓ is the total number of the line segments in the RP. Although empirical studies have shown that S_{RP} is capable of identifying dynamical transitions, S_{RP} is negatively correlated with the maximum Lyapunov exponent $\lambda_{\max}$ for some cases [14]. As a given dynamical system changes from a nonchaotic to a chaotic regime, it is expected that the entropy increases as well, since it is a measure of complexity, but this cannot always be observed with S_{RP} [2,14,23].

This unexpected behavior is the result of the following effect. When we consider, e.g., periodic dynamics, the RP should, in principle, consist of infinitely long diagonal lines. However, due to the finite time series length, these diagonal lines are cut at the borders of the RP, finally resulting in their different lengths, depending on their distance to the LOI, and hence increasing artificially the entropy measure. This biasing effect can also happen for nonperiodic dynamics as long as a significant number of diagonals cross the border of the RP. For chaotic dynamics, a majority of diagonal lines is not cut by the RP border, therefore, the bias in the entropy is negligible. Furthermore, the entropy measure also depends on the number of diagonal lines in the RP (i.e., indirectly on the recurrence threshold and the time series length), regardless of their length distribution. One way to overcome these problems is a correction scheme as suggested by [23]. However, it implies additional computational costs due to normalizing the line lengths depending on their distance to the LOI and normalizing the entropy by the number of diagonal lines.

Seeking an alternative descriptor for the dynamical complexity to be derived from RPs, another study has suggested the calculation of the Shannon entropy of the length distribution of diagonal segments of the nonrecurrence points (white dots) instead of the diagonal lines formed from the recurrence points (black dots) [19]. In other words, let $P_{\mathrm{white}}(\ell)$ be the number of connected diagonal nonrecurrence segments. In

order to compute the $P_{\text{white}}(\ell)$ histogram, we define a different recurrence matrix for white points $R^{\text{white}}_{i,j}$ as

$$R^{\text{white}}_{i,j} = 1 - R_{i,j}. \tag{4}$$

Using the $R^{\text{white}}_{i,j}$ matrix, we can compute the histogram $P_{\text{white}}(\ell)$ of diagonal lines of length ℓ as

$$P_{\text{white}}(\ell) = \sum_{i,j=1}^{N-1} \left(1 - R^{\text{white}}_{i-1,j-1}\right)\left(1 - R^{\text{white}}_{i+\ell,j+\ell}\right) \prod_{k=0}^{\ell-1} R^{\text{white}}_{i+k,j+k}. \tag{5}$$

The entropy measure is then defined as [19]

$$S^{\text{white}}_{\text{RP}} = -\sum_{\ell=\ell_{\min}}^{\ell_{\max}} p_{\text{white}}(\ell) \ln p_{\text{white}}(\ell), \tag{6}$$

where $p_{\text{white}}(\ell) = P_{\text{white}}(\ell)/N_{\text{white}}$ and N_{white} is the total number of the nonrecurrence line segments in the RP. In contrast to the results presented in [19], here we show that this entropy definition does not solve the problem of the anticorrelation between $S^{\text{white}}_{\text{RP}}$ and $\lambda_{\max}$.

In addition to the entropy definitions based on the length of line segments ℓ, it is worth mentioning that we can also define entropic measures through the distribution of time returns in RPs. An example is the recurrence probability density entropy [16], which measures the uncertainty associated with the distribution $P(T)$, where T is the recurrence time. Moreover, the Kolmogorov-Sinai entropy has also been generalized in the context of RPs in order to measure the complexity in the distribution of time returns [17].

In order to provide a more intuitive RP-based entropy measure, without anticorrelations with $\lambda_{\max}$, we propose a generalization of a weighted RP. Instead of considering a binary recurrence matrix, we take into account weights derived from the distance matrix $W_{i,j} = \|\mathbf{x}_i - \mathbf{x}_j\|$. Note that the binary matrix $\mathbf{R}$ provides information on whether or not two points i and j are close in a d-dimensional phase space, whereas $\mathbf{W}$ represents the distances between pairs of points of the time series (sometimes also referred to as an unthresholded RP [24]). In order to consider the proximity between points of the time series, we introduce the weight matrix

$$\widetilde{W}_{i,j} = e^{-\|\mathbf{x}_i - \mathbf{x}_j\|}, \tag{7}$$

which will be the base for our further analysis [Fig. 1(c)]. As particular weights $\widetilde{W}_{i,j}$ we have chosen the inverse of the exponential distribution because it scales the distances to the value range $[0, 1]$, with the value 1 for close states and 0 for distant states. For example, periodic regimes with the occurrence of identical states at i and $j = 2\pi k i$ result in $\widetilde{W}_{i,j} = 1$, whereas for diverging states with large distances $\widetilde{W}_{i,j}$ will tend to zero.

This definition of proximity comes with an additional benefit, i.e., it does not require selection of the recurrence threshold ε [as necessary for the other definitions (3) and (6)]. The selection of this threshold is not straightforward and a general method is not available yet [25].

Based on $\widetilde{\mathbf{W}}$, we propose the following recurrence-based entropy measure. We define the strength s_i of a point i in the time series by

$$s_i = \sum_{j=1}^{N} \widetilde{W}_{ij}. \tag{8}$$

In this way, the strength s_i quantifying the heterogeneity of the density of a given point in the phase space allows us to characterize the amount of statistical disorder in the system through its distribution $P(s)$. Therefore, the heterogeneity of the distance matrix $\widetilde{\mathbf{W}}$ can be calculated by its associated Shannon entropy, i.e.,

$$S_{\text{WRP}} = -\sum_{\{s\}} p(s) \ln p(s), \tag{9}$$

where $p(s) = P(s)/S$ is the relative frequency distribution of the distance matrix strength and $S = \sum_i^N s_i$ is the total number of strengths.

This alternative definition of RP-based entropy has the following differences with respect to the standard RP-based definition of the entropy (3). Instead of measuring the complexity of distributions $p(\ell)$ of diagonals, S_{WRP} measures the complexity of scalar distributions (the strength s_i) for each time point. Therefore, we get rid of the border effect that results in deceptive entropy values for S_{RP}. Moreover, as the calculation for S_{WRP} considers all time points, the results are not biased by the number of diagonals, therefore the time series length and the recurrence threshold are not crucial as in the S_{RP} case (the threshold is even unnecessary because we do not need to apply a threshold here). Instead, the value of S_{WRP} depends on the estimation of $p(s)$, i.e., the chosen binning.

For periodic or stochastic dynamics, the strength s_i will be very similar for all time points i, resulting in a confined distribution of $p(s)$ and finally a very low entropy value S_{WRP}. For chaotic dynamics, the strength s_i will vary strongly for different time points i, therefore the distribution $p(s)$ will be broad and S_{WRP} will increase. Thereby, S_{WRP} will be more correlated with the Lyapunov exponent than the diagonal-based entropies S_{RP} and $S^{\text{white}}_{\text{RP}}$.

III. COMPARISON OF THE ENTROPIES

In this section we compare the entropies [Eqs. (3), (6), and (9)] on simulated data, namely, the logistic map as a discrete case and the Rössler oscillator as a continuous one, and on experimental electrochemical data.

A. Logistic map

Mathematically, the logistic map is written

$$x_{i+1} = a x_i (1 - x_i), \tag{10}$$

where x_i is a real number between zero and one and a is a positive constant. We analyze the logistic map within the interesting range of the control parameter $a \in [3.5,4.0]$ with a step size of $\Delta a = 0.0005$. In this range, the logistic map shows rich dynamics, e.g., periodic and chaotic states, bifurcations, and inner and outer crises. For each value of a, we compute a time series of length $N = 5000$. In order to discard transients, we use only the last 3000 values of this time series. It was shown that RQA measures can distinguish different

dynamical behavior of the systems, such as chaos-period and chaos-chaos transitions [14,15]. As mentioned before, entropy quantifies the disorder of the system. Thus, we would expect that with an increasing chaotic nature of the system (i.e., increasing maximal Lyapunov exponent $\lambda_{\max}$), the entropy values should increase. However, within periodic windows, the entropy should significantly decrease.

For our study, we calculate the distance matrix and the RP without embedding. For the logistic map, larger values of the embedding dimension, i.e., dimension $m = 2$ or 3 and a delay of $\tau = 1$, do not change the result significantly because the logistic map is one dimensional. The selection of the recurrence threshold ε is crucial. Hence, in order to choose an optimal threshold, we use the recurrence rate method [2], i.e., selecting ε in such a way that the recurrence rate is constant at 5%. Sufficient small values of ε decrease the recurrence point density in RPs and lead to a better distinction of small variations, whereas larger values cause denser RPs but the sensitivity to detect small variations decreases. Weighted RPs, as mentioned before, do not depend on the threshold value ε.

Now we compare the entropies S_{WRP}, S_{RP}, and $S_{\mathrm{RP}}^{\mathrm{white}}$. Note that, in order to calculate S_{WRP}, 50 bins are used to derive the probability density function of strengths $p(s)$. We mainly find that the diagonal line entropy S_{RP} detects the transitions from periodic to chaotic and chaotic to periodic states. However, its correlation with the maximum Lyapunov exponent $\lambda_{\max}$ is opposite to what would be expected as mentioned before. Moreover, the values within periodic windows are not consistent, e.g., for $a \in [3.50,3.54]$ and $a \in [3.82,3.85]$, S_{RP} is larger than during chaotic regimes, but for periodic windows at $a \in [3.2\ldots]$ or $a \in [3.75\ldots]$, S_{RP} falls to zero [see Fig. 2(b)].

Similarly, the general trend of $S_{\mathrm{RP}}^{\mathrm{white}}$ is also anticorrelated to $\lambda_{\max}$ [Fig. 2(c)]. In the larger periodic windows $a \in [3.5,3.568]$ and $a \in [3.82,3.85]$, $S_{\mathrm{RP}}^{\mathrm{white}}$ has the highest values. However, the smaller periodic windows tend to have small $S_{\mathrm{RP}}^{\mathrm{white}}$.

In contrast, the weighted RPs entropy S_{WRP} is in general positively correlated with the maximum Lyapunov exponent of the logistic map throughout the entire range of the bifurcation parameter a. Within periodic states, $S_{\mathrm{WRP}}(s)$ has lower values and during chaotic regimes, it has higher values [Fig. 2(b)]. At the critical values of $a = 3.544$, 3.564, 3.630, 3.741, and 3.841, $S_{\mathrm{WRP}}(s)$ reveals sharp jumps.

In order to quantify the correlation between the entropies (S_{RP}, $S_{\mathrm{RP}}^{\mathrm{white}}$, and S_{WRP}) and the Lyapunov exponent $\lambda_{\max}$, the Pearson correlation coefficient is used,

$$\rho_{xy} = \frac{\mathrm{cov}(x,y)}{\sigma_x \sigma_y}, \tag{11}$$

where $\mathrm{cov}(x,y)$ is the covariance of two time series x and y and σ_x and σ_y are their standard deviations, respectively. As we can see from Table I, $S_{\mathrm{RP}}(\ell)$ and $S_{\mathrm{RP}}^{\mathrm{white}}(\ell)$ are anticorrelated with the Lyapunov exponent. On the other hand, $S_{\mathrm{WRP}}(s)$ is positively correlated with the Lyapunov exponent. Moreover, the absolute value of the correlation coefficients of the diagonal-line-based entropies is less than that of the weighted RP entropy.

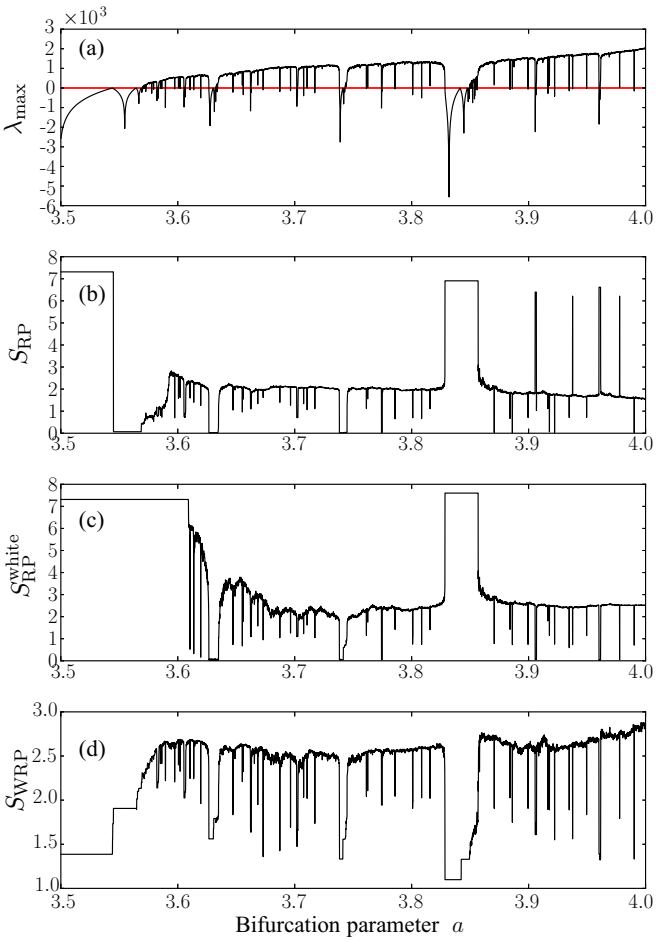

FIG. 2. (Color online) Comparison between (a) the Lyapunov exponent $\lambda_{\max}$, (b) $S_{\mathrm{RP}}(\ell)$ [Eq. (3)], (c) $S_{\mathrm{RP}}^{\mathrm{white}}$ [Eq. (6)], and (d) S_{WRP} [Eq. (9)] for the logistic map.

B. Rössler oscillator

Next we compare the different definitions of Shannon entropy applied on a time series from a continuous system, the Rössler oscillators [26]

$$\left(\frac{dx}{dt}, \frac{dy}{dt}, \frac{dz}{dt}\right) = (-y - z, x + ay, b + zc), \tag{12}$$

where the bifurcation parameter is $b \in [0.0,2.0]$ and the other parameters are $a = 0.2$ and $c = 5.7$. Here we analyze the Poincaré section of the y component of the Rössler oscillator. Contrary to the logistic map, increasing the control parameter b drives the system from chaotic states to periodic ones [Fig. 3(a)]. For each b value, we create a time series of the length $N = 6 \times 10^5$ and exclude the transient responses

TABLE I. Correlation between entropies and the Lyapunov exponent $\lambda_{\max}$ for the logistic map.

ρ_{xy}	$\lambda_{\max}$
$S_{\mathrm{RP}}(\ell)$	−0.52
$S_{\mathrm{RP}}^{\mathrm{white}}(\ell)$	−0.67
$S_{\mathrm{WRP}}(s)$	0.85

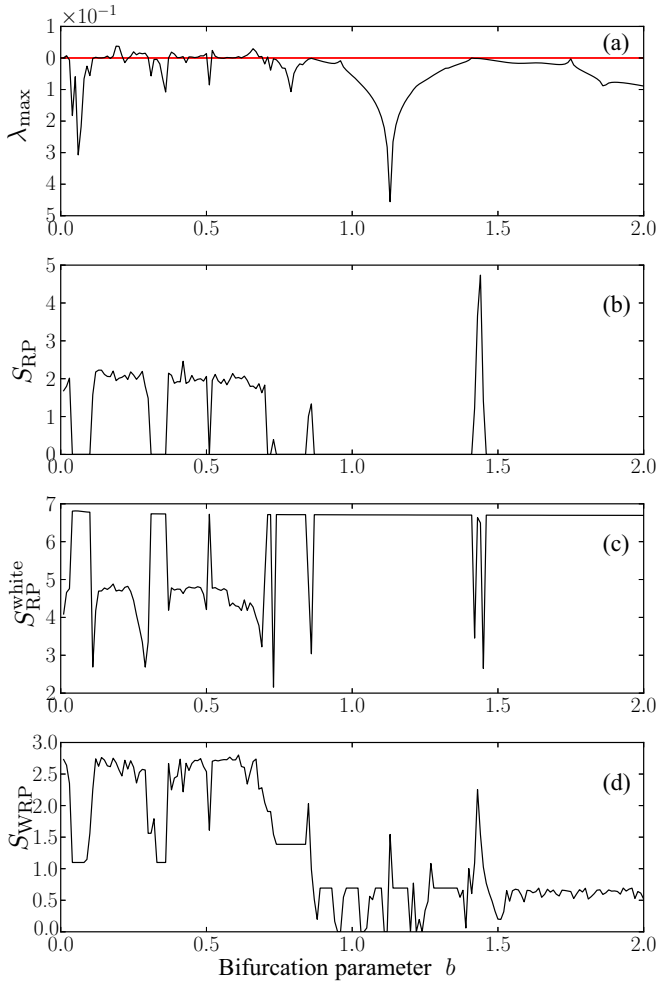

FIG. 3. (Color online) Comparison between (a) the Lyapunov exponent $\lambda_{\max}$, (b) $S_{\mathrm{RP}}(\ell)$ [Eq. (3)], (c) $S_{\mathrm{RP}}^{\mathrm{white}}$ [Eq. (6)], and (d) S_{WRP} [Eq. (9)] for the Rössler oscillator.

by using only the last 5×10^4 data points for the following analysis. We apply the Poincaré section on the phase space and use only the inner points of the Poincaré section to calculate **W** and **R** and to estimate the Shannon entropies. For each control parameter b, approximately 1000 inner points of the Poincaré section are used to compute the RPs. In order to calculate S_{WRP}, we also use 50 bins to construct the probability density function of strengths $p(s)$ as in the logistic map case.

We estimate the different entropies for the Rössler oscillations analogously to the logistic map. Although S_{RP} is anticorrelated for the logistic map case, this measure is correlated up to some degree with the Lyapunov exponent of the Rössler oscillator [Fig. 3(b)]. The entropy has higher values for the chaotic states and lower values for the periodic ones. A similar behavior can be observed for S_{WRP} [Fig. 3(d)]; S_{WRP} is also positively correlated with the Lyapunov exponent $\lambda_{\max}$.

However, the entropy $S_{\mathrm{RP}}^{\mathrm{white}}$, based on nonrecurrence line segments, reveals a different behavior. The general tendency is similar to the findings in the logistic map example: During periodic regimes, $S_{\mathrm{RP}}^{\mathrm{white}}$ is higher than during the chaotic regimes [Fig. 3(c)], in contrast to S_{RP} and S_{WRP}, which presented a similar dependence on b.

C. Application to electrochemical experiments

In this section we compare the three entropy definitions applied to experimental data from electrochemistry. The goal is to demonstrate the capability of the RP framework to grasp the complexity of patterns emerging from a real process. The kinetics of nickel electrodissolution include charge transfer steps that exhibit negative differential resistance (NDR); this NDR behavior generates a range of nonlinear behavior in which the rate of metal dissolution (current) exhibits simple and complex periodic and chaotic behavior [27–29]. We employed 30 nickel wires (1 mm diameter) as working electrodes in an electrochemical cell with $Hg/Hg_2SO_4/(sat)K_2SO_4$ reference and a Pt-coated Ti-rod counterelectrode in 4.5M sulfuric acid solution at 10 °C. The Ni wires were connected through 1.2-kΩ external resistances to a potentiostat (GillAC, ACM Instruments) that maintains constant circuit potential (V). The current time series for each wire (oscillator) is digitized at a rate of 200 Hz. Previous investigations showed that in this configuration there is negligible coupling among the wires and the oscillators can be regarded as independent [30]. In addition, there exists an inherent heterogeneity due to varying surface conditions that creates a population of oscillators with slightly different dynamical characteristics, e.g., there is a frequency distribution with a range of about 10–20 mHz [30]. The potential was incrementally increased by 10 mV from 1.3 to 1.4 V and about 1000 oscillations were collected at each potential. The frequency of the oscillations changed from 1.9 Hz (1.3 V) to 1.8 Hz (1.4 V). The transition from simple periodic oscillations through complex oscillations to chaotic oscillations and back to complex oscillations was visually observed with an increase of the potential. Inspection of the data reveals that the waveform of oscillations is preeminently period-1 (1.30–1.33 V) (P1), period-4 (1.34–1.35 V), chaos (1.36–1.39 V), and period-3 (1.4 V) (P3). These data are

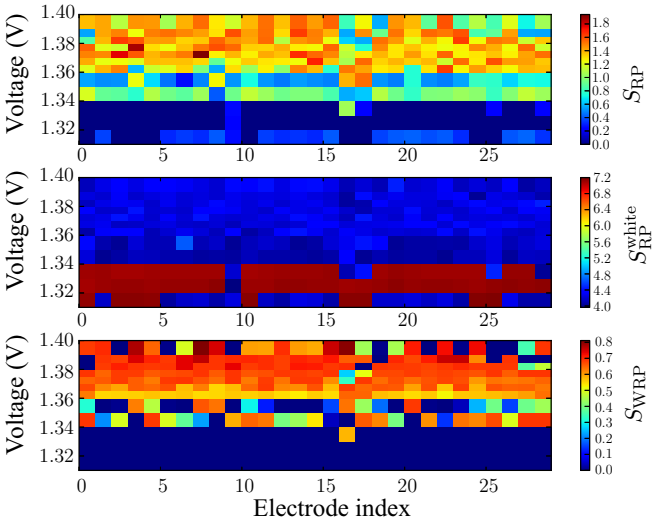

FIG. 4. (Color online) Complexity measures for 30 electrochemical oscillators as a function of circuit voltage. Color maps shows the entropies associated with the time series of each electrode for different values of voltage. The top shows the entropy S_{RP} of black dots [Eq. (3)], the middle the entropy of white dots $S_{\mathrm{RP}}^{\mathrm{white}}$ [Eq. (6)], and the bottom the entropy of weighted RPs S_{WRP} [Eq. (9)].

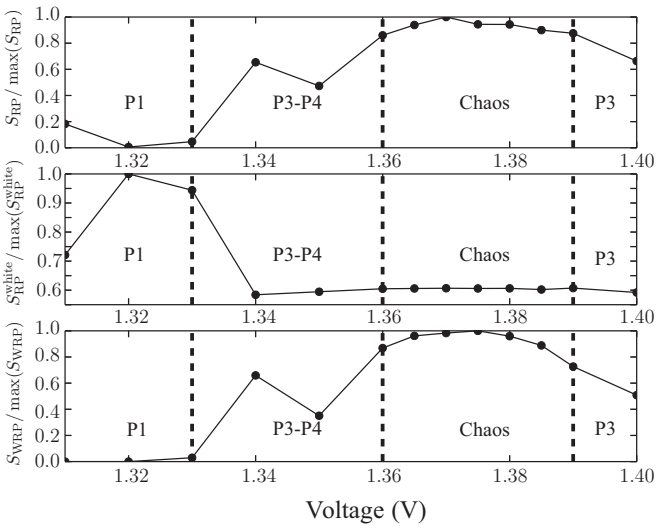

FIG. 5. Experimental results showing the comparison between the mean of the three normalized entropies over all electrodes for each value of the voltage. The top shows the entropy S_{RP} of black dots [Eq. (3)], the middle the entropy of white dots S_{RP}^{white} [Eq. (6)], and the bottom the entropy of weighted RPs S_{WRP} [Eq. (9)]. Again, 50 bins were considered to obtain the probability density function of strengths $p(s)$.

consistent with previous observation that a complex behavior is generated with a period-doubling bifurcation to chaos with the presence of intermittent periodic windows [27,29].

Figure 4 shows the results for the three recurrence entropy definitions applied to the time series obtained through the experiments described above. The system is expected to present oscillatory behavior for voltage values in the range [1.30 V,1.35 V] and therefore to present lower values of entropy measures. Similarly to the logistic map and the Rössler oscillator cases, again the entropy of white dots S_{RM}^{white} shows higher values for ranges in which the system is in a periodic regime, contrary to the expected scenario. On the other hand, the weighted entropy S_{WRP} and the entropy of black dots S_{RP} present a similar evolution as a function of the voltage applied, i.e., higher values in ranges in which the system is expected to present a chaotic behavior. Moreover, as we can see from Fig. 4, S_{WRP} is observed to have fewer fluctuations than S_{RP} for voltages below 1.34 V.

In Fig. 5 we present the electrode recurrence-based normalized entropy for each value of voltage averaged for the 30 oscillators. Because of the average, the trends in the changes of the entropies are better seen as the circuit potential is varied. It is easier to see the trend of the entropies due to the changing voltage of the system. Moreover, S_{RP}^{white} presents no correlated result with the dynamical regimes. Although the entropies of RPs and weighted RPs seem to be correlated with the dynamical regimes, S_{WRP} has more consistent values for the simple periodic case (P1).

Overall, we conclude that the S_{WRP} is suitable to reveal the complexity of the chemical reaction process; it has normalized values less than 0.2 for simple periodic oscillations, 0.2–0.7 for complex periodic (e.g., periods 4 and 3) oscillations, and larger than 0.7 for chaotic oscillations.

IV. CONCLUSION

We have presented a recurrence-based matrix to quantify the dynamical properties of a given system. The Shannon entropy of the recurrence matrix has been defined as a complexity measure and compared with the Shannon entropy of other recurrence-based approaches. Although entropy is a well known measure of disorder, in recurrence plot terminology, entropy is determined as a heuristic measure, in order to detect the transitions between different regimes. The probability of occurrence of diagonal line segments of different lengths is not equal since a recurrence plot is a square matrix whose dimension is limited by the length of the time series. The Shannon entropy is computed from the diagonal line distribution in the RP approach. Hence, the commonly adopted entropic measures based on line segments can often yield counterintuitive results when quantifying the complexity of a given system. This was exemplified with the logistic map case in which the entropy of black and white dots was observed to be anticorrelated with the Lyapunov exponent. On the other hand, the entropy of weighted RPs presented here recovered the expected dependence as a function of the system's complexity, i.e., showing higher values within regions in which chaos is observed. Moreover, for the continuous systems such as the Rössler attractor and experimental time series of electrochemical oscillators, although black dots and weighted entropies are both positively correlated with the emergence of chaotic behavior, the latter definition was observed to have more stable values for voltage ranges that lead to periodic time series. The ideas presented here can be extended and applied to other complex systems with the potential to better identify dynamical transitions in time series originating from them.

ACKNOWLEDGMENTS

D.E. and N.M. acknowledge support from the Leibniz Association (WGL) under Grant No. SAW-2013-IZW-2. T.K.D.M.P. would like to acknowledge FAPESP (Grant No. 2012/22160-7) and IRTG Grant No. 1740 (DFG and FAPESP). F.A.R. acknowledge CNPq (Grant No. 305940/2010-4), FAPESP (Grant No. 2011/50761-2 and No. 2013/26416-9), and NAP eScience–PRP–USP for financial support. L.d.F. Costa thanks CNPq (Grant No. 307333/2013-2), FAPESP (Grant No. 2011/50761-2), and NAP-PRP-USP for support. I.Z.K. acknowledges support from the National Science Foundation under Grant No. CHE-0955555 and SLU PRF. J.K. would like to acknowledge IRTG Grant No. 1740 (DFG and FAPESP) for the sponsorship provided.

[1] J.-P. Eckmann, S. Oliffson Kamphorst, and D. Ruelle, Europhys. Lett. **4**, 973 (1987).

[2] N. Marwan, M. Carmen Romano, M. Thiel, and J. Kurths, Phys. Rep. **438**, 237 (2007).

[3] M. A. Riley and S. Clark, Neurosci. Lett. **342**, 45 (2003).
[4] S. Schinkel, N. Marwan, and J. Kurths, J. Physiol. (Paris) **103**, 315 (2009).
[5] S. Carrubba, C. Frilot II, A. L. Chesson, Jr., and A. A. Marino, Neurosci. Lett. **469**, 164 (2010).
[6] N. Marwan, M. H. Trauth, M. Vuille, and J. Kurths, Clim. Dynam. **21**, 317 (2003).
[7] W. von Bloh, M. C. Romano, and M. Thiel, Nonlinear Process. Geophys. **12**, 471 (2005).
[8] T. Matcharashvili, T. Chelidze, and J. Peinke, Nonlinear Dynam. **51**, 399 (2008).
[9] J. F. Donges, R. V. Donner, M. H. Trauth, N. Marwan, H. J. Schellnhuber, and J. Kurths, Proc. Natl. Acad. Sci. USA **108**, 20422 (2011).
[10] H. Voss, J. Kurths, and U. Schwarz, J. Geophys. Res. **101**, 15637 (1996).
[11] N. Asghari, C. Broeg, L. Carone, R. Casas-Miranda, J. C. C. Palacio, I. Csillik, R. Dvorak, F. Freistetter, G. Hadjivantsides, H. Hussmann, *et al.*, Astron. Astrophys. **426**, 353 (2004).
[12] N. V. Zolotova, D. I. Ponyavin, N. Marwan, and J. Kurths, Astron. Astrophys. **505**, 197 (2009).
[13] N. Marwan, Eur. Phys. J. Spec. Top. **164**, 3 (2008).
[14] L. Trulla, A. Giuliani, J. Zbilut, and C. Webber, Phys. Lett. A **223**, 255 (1996).
[15] N. Marwan, N. Wessel, U. Meyerfeldt, A. Schirdewan, and J. Kurths, Phys. Rev. E **66**, 026702 (2002).
[16] L. M. Little, P. McSharry, S. J. Roberts, D. A. E. Costello, and I. M. Moroz, BioMed. Eng. Online **6**, 23 (2007).
[17] M. S. Baptista, E. J. Ngamga, P. R. F. Pinto, M. Brito, and J. Kurths, Phys. Lett. A **374**, 1135 (2010).
[18] E. J. Ngamga, D. V. Senthilkumar, and J. Kurths, Eur. Phys. J. Spec. Top. **191**, 15 (2010).
[19] C. Letellier, Phys. Rev. Lett. **96**, 254102 (2006).
[20] N. H. Packard, J. P. Crutchfield, J. D. Farmer, and R. S. Shaw, Phys. Rev. Lett. **45**, 712 (1980).
[21] H. Kantz and T. Schreiber, *Nonlinear Time Series Analysis* (Cambridge University Press, Cambridge, 1997).
[22] M. Thiel, M. C. Romano, P. L. Read, and J. Kurths, Chaos **14**, 234 (2004).
[23] F. Censi, G. Calcagnini, and S. Cerutti, IEEE Trans. Biomed. Eng. **51**, 856 (2004).
[24] A. Sipers, P. Born, and R. Peeters, Phys. Lett. A **375**, 2309 (2011).
[25] N. Marwan, Int. J. Bifurcat. Chaos **21**, 1003 (2011).
[26] O. E. Rössler, Phys. Lett. A **57**, 397 (1976).
[27] O. Lev, A. Wolffberg, L. M. Pismen, and M. Sheintuch, J. Phys. Chem. **93**, 1661 (1989).
[28] I. Z. Kiss, Y. Zhai, and J. L. Hudson, Science **296**, 1676 (2002).
[29] I. Z. Kiss, W. Wang, and J. L. Hudson, Phys. Chem. Chem. Phys. **2**, 3847 (2000).
[30] M. T. M. Koper, Adv. Chem. Phys. **92**, 161 (1996).